Reevaluating the Hartman effect for field emission

Kevin L. Jensen* and Andrew Shabaev
Code 6362, Naval Research Laboratory, Washington, DC 20375, USA

Jeanne Riga and Donald A. Shiffler
Directed Energy Directorate, Air Force Research Laboratory, Albuquerque, New Mexico 87117, USA

Joel L. Lebowitz
Departments of Mathematics and Physics, Rutgers University, Piscataway, New Jersey 08854, USA

Rebecca Seviour
School of Computing and Engineering, University of Huddersfield, Huddersfield HD1 3DH, United Kingdom

(Received 30 July 2021; accepted 19 November 2021; published 9 December 2021)

An electron wave packet tunneling through a barrier has a transmission (or "group delay") time τ_g that, for a rectangular barrier, is commonly held to become independent of the barrier width L as the width increases (the *McColl-Hartman effect*). In the present study, it is shown that first, the McColl-Hartman effect for a rectangular barrier is dependent upon L as the Gamow tunneling factor $\theta(k)$ vanishes, and τ_g is only independent of L when $\theta(k)$ is large; and second, for a triangular barrier to model field emission, although τ_g can be large for small field, it vanishes when the energy matches the barrier height.

DOI: 10.1103/PhysRevA.104.062203

I. INTRODUCTION

The question of how long an electron spends tunneling through a barrier has taken on increasing importance for nanogap devices [1–6] such as nanoantennas for which field emission occurs across an anode-cathode (AK) gap of 50 nm [7] down to 8 nm [8] (where the anode-cathode transit time [9] is on the order of femtoseconds), and attosecond experiments [10–12]. In his consequential study of tunneling across thin insulating layers using a model for which an incident wave packet encounters a rectangular barrier, Hartman [13] and earlier McColl [14] found that the transmission time for a metal-insulator-metal (MIM) thin film was given by the group delay $\tau_g = \hbar/\sqrt{\mu\Phi}$ in the limit of large barrier width, where μ is the Fermi level and Φ is the vacuum work function: for a generic case where $\mu = \Phi = 1$ eV, then $\tau_g = 0.658\,21$ fs and, parenthetically, is smaller than but comparable to the barrier width-dependent semiclassical time of Büttiker and Landauer [15] of $\tau_{sc} = L/\sqrt{2\Phi/m} = 1.6860$ fs for $L = 1$ nm, but of a very different nature as demonstrated by Winful [16,17], who demonstrated that τ_g was the sum of a dwell τ_d and self-interference τ_i time.

Our study of wave-packet interactions with barriers using a time-dependent Wigner distribution function (WDF) approach [18] indicates that rectangular barriers (and others with similar abrupt transition behavior) have properties that make their usage for wave packets problematic for simulations, even though plane-wave and exponentially growing/decaying solutions are highly advantageous. Specifically, wave packets of finite momentum spread contain $k > k_v$ contributions, where $\hbar^2 k_v^2/2m = V_o = \mu + \Phi$ is the barrier height. In the $L\kappa \gg 1$ limit where $\kappa = \sqrt{k^2 - k_v^2}$, the sine functions in the transmission probability $D_{\text{rec}}(k)$ become highly oscillatory and possess numerous peaks $[D(k_n) = 1]$ where $L\sqrt{k_n^2 - k_v^2} = \pi n$ for n integer [19]. This is in sharp contrast to the step barrier for which $D_{\text{step}}(k) = 4k\kappa/(k+\kappa)^2$ asymptotically approaches unity. A model that smoothly and asymptotically approaches the step limit is preferable for modeling field emission. The present study provides it in the following steps. First, as per Winful, attention is explicitly restricted to energy eigenstates $\psi_k(x)$ (not wave packets). Second, the analysis of Winful is recast using the Gamow factor $\theta(k)$ to allow generalization. Third, the Gamow analysis is repeated for a barrier characteristic of high-field electron emission. Several candidates are available: (i) The image charge or Schottky-Nordheim (SN) barrier [20] describes field emission from metals [21] and semiconductors [22] and has a semianalytic Gamow factor $\theta(k)$, but the transmission $t(k)$ and reflection $r(k)$ coefficients must be calculated numerically; (ii) the Eckart barrier [23] is an asymmetric barrier for which $t(k)$ and $r(k)$ are analytic, but the Gamow factor $\theta(k)$ must be calculated numerically; and (iii) the triangular or Fowler-Nordheim (FN) barrier [21] for field emission neglects image charge effects but $t(k)$, $r(k)$, and $\theta(k)$ are all completely analytic. Therefore, only the triangular barrier of choice (iii) is a simple and purely analytic representation of field emission under high-field conditions (and is the most iconic example of tunneling wave mechanics [24,25]). Thus, the FN formalism [26–28] is used for the development and analysis of the dwell τ_d and self-interference τ_i times.

*kjensen@mailaps.org

II. McCOLL-HARTMAN EFFECT

The much discussed independence of τ_g on the width L of the rectangular barrier as L increases is termed the "Hartman effect": The dependence had been anticipated separately by McColl, so that the designation "McColl-Hartman" is preferable [29] and used herein. In Hartman's description, the time taken to traverse a barrier of width L is termed the "transmission time" τ_g. It becomes independent of L and small compared to the time taken for a packet to traverse the same distance in free space, known as the "equal time," in the limit $L \to \infty$. Hartman's observation has been expressed by others similarly: "The Hartman effect is the saturation of the group delay with barrier length" (Winful [16]); "Hartman observed that the transmission time approaches a constant for most energies less than the barrier height (except for energies *very close to the barrier height* or very close to zero)" (emphasis added, Smith and Blaylock [30]); "simple phase time following the calculation of Hartman turns out to be independent of the thickness a of the barriers..." (Petrillo and Olkhovsky [31]); and "the time taken to traverse a barrier appears to be independent of the length of the barrier when said barrier is sufficiently broad" (Rivlin *et al.* [29]). The implication is that if the time taken to traverse the barrier becomes constant (independent of L) in the wide barrier limit, then superluminal velocities are achieved, a conclusion that violates causality. In the following, propagation through some well-known barriers uses the Gamow factor, which depends upon both incident energy and barrier thickness. The resulting interpretation does not imply superluminal transport.

A. Rectangular barrier

The rectangular barrier is commonly used to simulate tunneling through a metal-insulator-metal (MIM) barrier. The rectangular barrier is given by

$$V_{\rm rec}(x) = V_o\Theta(x)\Theta(L-x) \equiv \frac{\hbar^2 k_v^2}{2m}\Theta(x)\Theta(L-x), \tag{1}$$

where $\Theta(x)$ is the Heaviside step function, $V_o = \mu + \Phi \equiv \hbar^2 k_v^2/2m$ is the barrier height, and L is the barrier width. Winful [16,17] demonstrates that τ_g is the sum of a dwell time τ_d and a self-interference time τ_i, respectively, given as [compare τ_d to Eq. (2) of Ref. [15]]

$$\tau_d(k) \equiv \left(\frac{m}{\hbar k}\right)\int_0^{L(k)} |\psi_k(x)|^2 dx, \tag{2}$$

$$\tau_i(k) \equiv -\frac{\hbar}{k}{\rm Im}[r(k)]\left(\frac{dk}{dE}\right), \tag{3}$$

$$\tau_g(k) \equiv \tau_d(k) + \tau_i(k), \tag{4}$$

where $\psi_k(x<0) = e^{ikx} + r(k)e^{-ikx}$ and $\psi_k(x>L) = t(k)e^{ikx}$, ${\rm Im}[r(k)]$ is the imaginary part of $r(k)$, $L(k)$ is the separation between where the wave function enters and emerges from a general barrier, $dk/dE = m/\hbar^2 k$, and $\hbar k$ is the momentum of the eigenstate. The transmission and reflection coefficients, $t(k)$ and $r(k)$, respectively, for $V_{\rm rec}(x)$ for $k > k_v$ are [28,32]

$$t_{\rm rec}(k) = \frac{2k\kappa e^{-ikL}}{2k\kappa\cos(L\kappa) - i(k^2+\kappa^2)\sin(L\kappa)},$$
$$r_{\rm rec}(k) = \frac{-i(k^2-\kappa^2)\sin(L\kappa)}{2k\kappa\cos(L\kappa) - i(k^2+\kappa^2)\sin(L\kappa)}, \tag{5}$$

where $\kappa(k) \equiv |k_v^2 - k^2|^{1/2}$ so that κ is chosen to *always* be real and positive. The transmission probability is then $D_{\rm rec}(k) = |t_{\rm rec}(k)|^2$; for over the barrier,

$$D_{\rm rec}(k>k_v) = \left\{1 + \left[\frac{1}{2}\left(\frac{k}{\kappa} - \frac{\kappa}{k}\right)\sin(L\kappa)\right]^2\right\}^{-1}. \tag{6}$$

For $k < k_v$ then $\kappa \to i\kappa$, causing the trigonometric terms to become their hyperbolic counterparts. The Gamow factor for $V_{\rm rec}(x)$ is given by $\theta(k) \equiv 2\sigma\kappa(k)L$, where the tunneling width L is constant and the shape factor $\sigma = 1$ [33,34]. Invoking half-angle formulas to convert $\cosh(\theta/2)$ and $\sinh(\theta/2)$ to easier forms, then for $k < k_v$,

$${\rm Im}[r(k)] = -\frac{2k\kappa k_v^2\sinh\theta}{k_v^4[\cosh\theta - 1] + 2(2k\kappa)^2}, \tag{7}$$

and therefore

$$\frac{\tau_i(k)}{\tau_o} = \left(\frac{\kappa k_v^4}{k}\right)\frac{\sinh\theta}{k_v^4(\cosh\theta - 1) + 2(2k\kappa)^2}, \tag{8}$$

where $\tau_o = \hbar/V_o$. $\tau_d(k)$ requires the coefficients of the wave function inside the barrier, where $\psi_k(x) = a(k)e^{-\kappa x} + b(k)e^{\kappa x}$. They are solutions to [28,32,35,36]

$$\begin{pmatrix} a(k) \\ b(k)\end{pmatrix} = \frac{1}{2\kappa}\begin{bmatrix}\kappa - ik & \kappa + ik \\ \kappa + ik & \kappa - ik\end{bmatrix}\begin{pmatrix}1 \\ r(k)\end{pmatrix}. \tag{9}$$

Insertion of $\psi_k(0<x<L)$ into Eq. (2) and using $\int_0^L e^{\pm 2\kappa x}dx = \pm(L/2)(e^{\pm\theta} - 1)/\theta$ results in

$$\frac{\tau_d(k)}{\tau_o} = \left(\frac{kk_v^2}{\kappa}\right)\frac{k_v^2\sinh\theta - (k^2-\kappa^2)\theta}{k_v^4(\cosh\theta - 1) + 2(2k\kappa)^2}. \tag{10}$$

Although the McColl-Hartman effect is conventionally taken as a wide barrier ($L \to \infty$) limit, here, it is the $\theta \to \infty$ limit because θ can be large even when κ is small. Therefore, for large θ, τ_d and τ_i are (compare Appendix D, Ref. [18])

$$\tau_d(k) = \tau_o\frac{k}{\kappa}\tanh\theta, \quad \tau_i(k) = \tau_o\frac{\kappa}{k}\tanh\theta, \tag{11}$$

so that $\tau_g = \tau_o(k_v^2/k\kappa)\tanh\theta$ is the sum, as per Eq. (4). Hartman's (and Winful's) finding that $\tau_g \to \tau_o k_v^2/k\kappa$ is then recovered when $\theta > 4$ for which $\tanh\theta$ differs from unity by $<0.07\%$. It should be noted that the transmission time in the limit of large barrier width and low energy is no longer a useful metric for measuring propagation time through the barrier because the transmission probability in that limit approaches zero as per Eq. (6). The reflection delay is a better metric, and does approach a constant value in the wide barrier limit.

However, when $k = k_v$ (or $E = V_o$), the Gamow factor vanishes even though L is finite and large. This entails that as $k \to k_v$, then the small θ limit is required. Expanding $\sinh\theta$ and $\cosh\theta$ for small θ, replacing $\theta = 2\kappa L$, and then taking the

limit $k \to k_v$ gives

$$\lim_{k\to k_v} \frac{\tau_d(k)}{\tau_o} = \frac{2Lk_v}{3}\left[\frac{(Lk_v)^2+3}{(Lk_v)^2+4}\right], \tag{12}$$

$$\lim_{k\to k_v} \frac{\tau_i(k)}{\tau_o} = \frac{Lk_v}{(Lk_v)^2+4}. \tag{13}$$

In the large L limit when $k = k_v$, then Hartman's result for τ_g, which would otherwise seemingly diverge as $1/\kappa(k)$, is instead

$$\lim_{L\to\infty} \frac{\tau_g(k_v)}{\tau_o} = \left(\frac{Lk_v}{3}\right)\frac{2(Lk_v)^2+9}{(Lk_v)^2+4} \to \frac{2}{3}Lk_v, \tag{14}$$

as per Eq. (4) and therefore *is not independent of the barrier width* L when $k = k_v$. Thus, the independence of barrier width is a large θ limit rather than a large L limit, an important distinction because θ vanishes for $k = k_v$, where $\tau_g(k_v) = \tau_d(k_v)$ are finite. The behavior of τ_d, τ_i, and τ_g are shown in Figs. 1 and 2 for increasing L.

B. Triangular barrier

Field emission from a fiber [37] or metal [20] requires a large electric field to initiate tunneling. This process can be elegantly and analytically represented using a triangular barrier model. First, the transmission probability for a triangular barrier does not oscillate as does Eq. (6), which becomes increasingly oscillatory as L increases. Furthermore, when $k > k_v$, the Airy function solutions to Schrödinger's equation behave such that $D_{fn}(k > k_v) \to 4k\kappa/(\kappa+k)^2$ when the applied field $\mathcal{E} \to 0$, which smoothly recovers the step function barrier. The triangular barrier is given by

$$V(x>0) = V_o - Fx \equiv \frac{\hbar^2}{2m}\left[k_v^2 - fx\right] \tag{15}$$

and zero for $x < 0$, where $F = q|\mathcal{E}|$ contains the electric field $\mathcal{E}$, and q is the (positive) elementary charge unit, so that the charge of an electron is $-q$. The tunneling length factor L is now dependent upon F in Eq. (15) [38], and therefore

$$L(k) = \frac{V_o - E}{F} = \frac{k_v^2 - k^2}{f} = \frac{\kappa(k)^2}{f} \tag{16}$$

for field emission conditions. For $x > 0$, $\psi_k(x) = t(k)[\mathrm{Ai}(w) - i\,\mathrm{Bi}(w)]$, where

$$w(x) = \frac{k_v^2 - k^2 - fx}{f^{2/3}}. \tag{17}$$

Using the asymptotic forms of the Airy functions, the transmission and reflection factors associated with the barrier of Eq. (15) lead to the self-interference time

$$\frac{\tau_i(k)}{\tau_o} = \frac{\pi f^{1/3}k_v^2\,\chi(\theta)}{k[\pi k^2\Sigma(\theta) + \pi f^{2/3}\Sigma'(\theta) + 2f^{1/3}k]}, \tag{18}$$

where for $k < k_v$, $\theta(k) = 4\kappa^3/3f = 2\sigma\kappa L$ for $\sigma = 2/3$ and $L(k) = \kappa^2/f$ [34], and

$$\begin{aligned}
\Sigma(\theta) &= \mathrm{Ai}[w(0)]^2 + \mathrm{Bi}[w(0)]^2,\\
\Sigma'(\theta) &= \mathrm{Ai}'[w(0)]^2 + \mathrm{Bi}'[w(0)]^2,\\
\chi(\theta) &= \mathrm{Ai}[w(0)]\,\mathrm{Ai}'[w(0)] + \mathrm{Bi}[w(0)]\,\mathrm{Bi}'[w(0)].
\end{aligned} \tag{19}$$

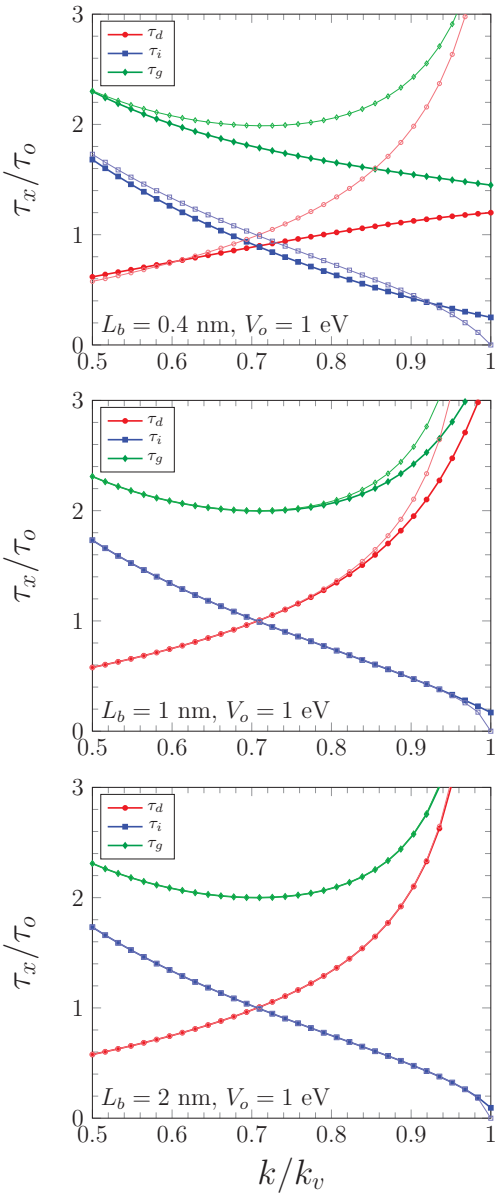

FIG. 1. Comparisons of rectangular barrier dwell time τ_d [Eq. (8), red •], self-interference delay τ_i [Eq. (10), blue ■], and group delay τ_g [Eq. (4), green ♦] to the asymptotic large-θ form [Eq. (11), thin light lines and ○, □, ◊, respectively] for increasing L (top to bottom).

The large and small θ limits have separate behavior. In the large θ limit, $\tau_i(k)$ becomes

$$\frac{\tau_i(k)}{\tau_o} \approx \frac{\kappa k_v^2}{k(k_v^2 + 2k\kappa e^{-\theta})} \tag{20}$$

and therefore approaches $\tau_i(k)/\tau_o \to \kappa/k$ as $\theta \to \infty$. In the $(k \to k_v)$ limit where $\theta \to 0$, $\tau_i(k)$ becomes

$$\begin{aligned}
\frac{\tau_i(k_v)}{\tau_o} &= \frac{\pi f^{1/3}k_v\,\chi(0)}{\pi k_v^2\Sigma(0) + \pi f^{2/3}\Sigma'(0) + 2f^{1/3}k_v}\\
&= \frac{\sqrt{3}\epsilon}{4\epsilon^2 + 6\epsilon + 3},
\end{aligned} \tag{21}$$

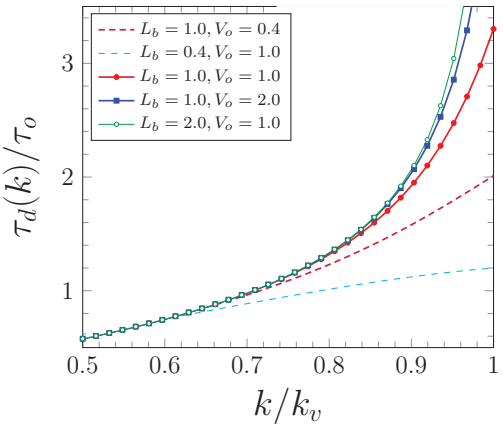

FIG. 2. The rectangular barrier dwell times $\tau_d(k)$ [Eq. (10)] for various barrier widths L and heights V_o: Larger values are associated with larger θ; the smallest two values are dashed lines.

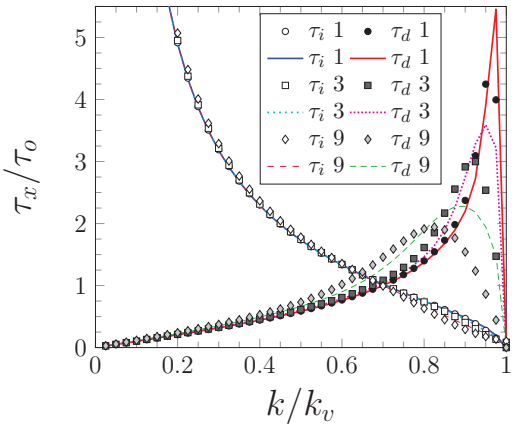

FIG. 3. Comparison of the exact ($\circ, \square, \Diamond$) $\tau_i(k)$ [Eq. (18)] and ($\bullet, \blacksquare, \blacklozenge$) $\tau_d(k)$ [Eq. (23)] to the approximations for τ_i/τ_d (thick blue line/thick red line = 1, loosely dotted cyan/densely dotted purple = 3, and loosely dashed magenta/densely dashed green = 9) of Eqs. (20) and (24), respectively. The legend is labeled by values of F (0.1 eV/nm). $V_o = 1.25$ eV and $\tau_o = 0.526\,57$ fs. The subscript x on the τ_x axis label denotes either d or i. τ_g (not shown) would be the sum as per Eq. (4). The curves for τ_i overlap so closely as to not be easily distinguishable.

where $\epsilon = f^{1/3}/\eta k_v$ where $\eta \equiv (4\pi/3)\,\mathrm{Bi}(0)^2 = 1.5839$. For finite F, $\tau_i(k_v)$ does not vanish. The behavior of $\tau_i(k)$ therefore mimics its analog for the rectangular barrier, where $f^{1/3}/\eta\sqrt{3}$ takes over the role of $1/L$.

The dwell time $\tau_d(k)$ makes use of

$$|\psi_k(x)|^2 = |t(k)|^2 \Sigma\left(\frac{4}{3}w(x)^{3/2}\right),$$

$$|t(k)|^2 = \frac{4\pi k^2}{\pi k^2 \Sigma(\theta) + \pi f^{2/3}\Sigma'(\theta) + 2kf^{1/3}}, \tag{22}$$

where $\theta \equiv 4\kappa^3/3f$ as before, from which

$$\frac{\tau_d(k)}{\tau_o} = |t(k)|^2 \frac{k_v^2}{2kf^{1/3}} \int_0^\theta \frac{\Sigma(u)}{u^{1/3}} du. \tag{23}$$

Again, the large and small θ limits of $\tau_d(k)$ have separate behavior. In the large θ limit

$$\frac{\tau_d(k)}{\tau_o} \approx \frac{5k_v^2\kappa}{4\pi k f^{2/3}} |t(k)|^2 [1 + \delta(\theta)], \tag{24}$$

$$\delta(\theta) \equiv \frac{1}{15\theta^{1/3}} \int_0^\theta \frac{e^{-z} + 4e^z - 5}{z^{2/3}} dz. \tag{25}$$

For large θ, $\delta \approx 4e^\theta/15\theta$ and $|t|^2 \approx 4\pi k^2 \kappa e^{-\theta}/f^{1/3}k_v^2$, so

$$\frac{\tau_d(k)}{\tau_o} \approx \frac{k_v^2 f^{1/3}}{4\pi k\kappa^2} |t(k)|^2 e^\theta = \frac{k}{\kappa}, \tag{26}$$

with the next order term going as $e^{-\theta}$, akin to Eq. (11). The large θ limit of τ_g is then the sum of Eqs. (21) and (24), as per Eq. (4). As with the large θ limit for the rectangular barrier, the reflection delay is again a better metric.

In the small θ limit, the integrand in Eq. (23) may use a polynomial expansion for the small argument of $\Sigma(u)$ from Eq. (19) and then integrated analytically term by term. It is found

$$\frac{\tau_d(k_v)}{\tau_o} \to |t(k_v)|^2 \left(\frac{\eta(k_v\kappa)^2}{2\pi f}\right)\left[1 + \frac{\kappa^2}{\sqrt{3}\eta f^{2/3}}\right], \tag{27}$$

which vanishes as κ^2 as $k \to k_v$ [compare Eq. (12)]. The behavior of $\tau_d(k)$ is therefore *in contrast to the behavior of its analog* for the rectangular barrier, where $\tau_d(k)$ remains finite as $k \to k_v$ for finite L. An evaluation of $\tau_i(k)$ and $\tau_d(k)$ is shown for several representative fields and barrier heights in Fig. 3 where, again, τ_g would be found as per Eq. (4). The larger $\theta(E) \propto (V_o - E)^{3/2}/F$ is, the better are the approximations. Notably, if applied to a wave packet composed of many components, and when either L or $1/f$ is large, then the more energetic components will increasingly constitute the outgoing packet, and they will therefore be associated with the smallest $\theta(k)$ factors. Efforts to bypass such complications by making very wide wave packets with very narrow momentum spreads entail complications for the simulation of tunneling that are difficult. The relations $\tau_d(k)$ and $\tau_i(k)$ to the WDF analysis of wave packets of our prior work shall be taken up separately.

III. OTHER BARRIERS

A visual comparison of Figs. 1 and 3 demonstrates similarities in the large θ limit, even though the underlying potential barriers represent extreme cases. Therefore, as the final step of the analysis, consider two more representative barriers. The Schottky-Nordheim (SN) barrier [27,28,39] describes field emission from metals and semiconductors by including image charge effects; it possesses an analytic θ but requires numerical evaluation for $t(k)$ and $r(k)$. The Eckart barrier is an asymmetric barrier which enables analytic $t(k)$ and $r(k)$ [23] but requires a numerical evaluation of θ. Both are treated in tandem with regards to θ and suggested to be compatible with Eq. (11) as was Eq. (26). A confirmation of this can be had using an exact Airy transfer matrix approach to solve Schrödinger's equation [34] so as to obtain $\psi_k(x)$ exactly, and shall be undertaken separately. Therefore, here, Gamow behavior with respect to the scale factor $\sigma \equiv \theta/2\kappa L$ is undertaken. In both cases, the expressions for the location x_o of the maximum of the barrier, $\kappa(E) \equiv \sqrt{2m|V(x_o) - E|}/\hbar$,

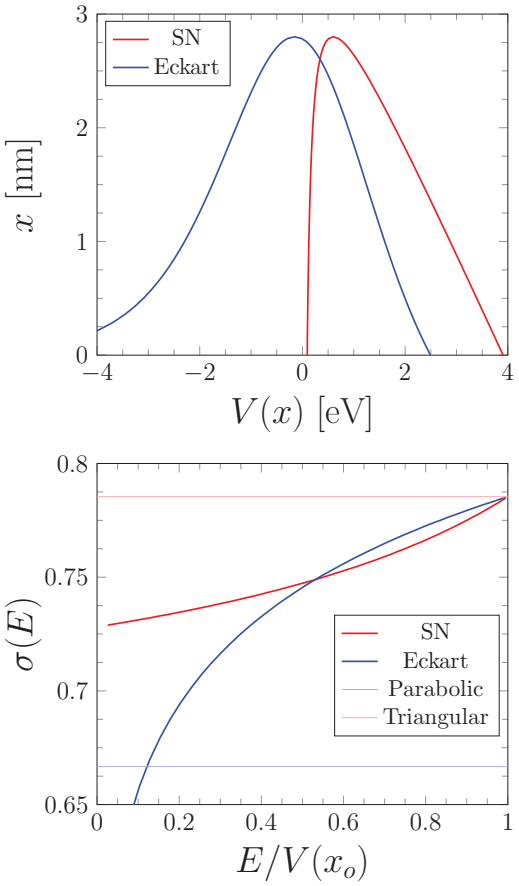

FIG. 4. Top: $V(x)$ for the SN and Eckart barriers for parameters in the text. Bottom: The resulting scale factor $\sigma(E)$ for each, where "Parabolic" and "Triangular" denote $\sigma(E) = (2/3, \pi/4)$ for the inverted parabolic and the triangular FN barriers, respectively, for which both are constant.

and the zeros $x_\pm(E)$ defined such that $V(x_\pm) - E = 0$ can be analytically found. Lastly,

$$\sigma(E) \equiv \int_{x_-}^{x_+} \left[\frac{V(x) - E}{V(x_o) - E}\right]^{1/2} \frac{dx}{x_+ - x_-} \tag{28}$$

defines the shape factor and is evaluated here numerically. The terms are accordingly given by the following:

(1) Schottky-Nordheim:

$$\begin{aligned} V_{sn}(x) &= \mu + \Phi - Fx - Q/x, \\ L(E) &= [\mu + \Phi - E)^2 - 4QF]^{1/2}/F, \\ x_\pm(E) &= [\mu + \Phi - E \pm FL(E)]/2F, \quad x_o = \sqrt{Q/F}, \end{aligned} \tag{29}$$

(2) Eckart:

$$\begin{aligned} V_e(x)/V_e(x_o) &= g(-x)[ag(x) - 1], \\ g(x) &= [\exp(x/b) + 1]^{-1}, \\ x_\pm(E) &= b \ln\left[\frac{(a-1)(1 \pm \delta)}{a + 1 \mp (a-1)\delta}\right], \\ x_o &= b \ln[(a-1)/(a+1)], \end{aligned} \tag{30}$$

where the parameters are chosen such that the Fermi level and work function are $\mu = \Phi = 2$ eV, the field is $F = 1$ eV/nm, the image charge term is $Q = 0.36$ eV nm, $b = 1$ nm, $a = 1 + 2(\mu + \Phi) + 2\sqrt{(\mu + \Phi)(\mu + \Phi + 1)}$ is chosen so that the maximum of the barriers is the same, and δ is such that $E/V(x_o) = 1 - \delta^2$. The comparisons are shown in Fig. 4. Although the shape factors are calculated here numerically for consistency and accuracy, it is known that in the case of the Schottkty-Nordheim (SN) barrier, the shape factor evaluated at the Fermi level $E = \mu$ is related to the Schottky-Nordheim function $v(y)$ [40] by the relation [Eq. (B3) of Ref. [34]]

$$v(y) = \tfrac{3}{2}(1 - y)\sqrt{1 + y}\,\sigma_{sn}(\mu), \tag{31}$$

where $y(\mu) \equiv \sqrt{4QF}/\Phi$ and $v(y) \approx 1 - y^2[1 - \ln(y)/3]$ is the approximation due to Forbes and Deane [27]. Note that $y(\mu)$ is a special case of $y(E) = [\mu + \Phi - V(x_o)]/(\mu + \Phi - E)$ for the Schottky-Nordheim barrier.

The numerical comparisons of $\sigma(E)$ as E varies from zero to the barrier maximum are shown in Fig. 4, for energy measured with respect to the conduction-band minimum of the left contact. It is seen that the SN barrier stays closer to the triangular barrier (FN) case, but the Eckart potential moves closer to the parabolic case as E decreases. Interestingly, for energies closer to the barrier maximum, both SN and Eckart result in σ values that are reasonably close. The consequences on θ and therefore τ_d are taken up separately.

IV. CONCLUSION

In summary, the behaviors of the self-interference τ_i and dwell τ_d times that make up the group delay as per Winful [16,17] have been reevaluated for the rectangular (or MIM) barrier and extended to the triangular (or field emission) barrier. For the rectangular barrier, the oft made claim that the delay time becomes sensibly independent of the width L of the barrier (the McColl-Hartman effect) applies *only* to conditions where the Gamow factor $\theta(k)$ is large [e.g., where $k < \sqrt{k_v^2 - (2/L)^2}$]: When θ is small, then the dwell and self-interference times are in fact dependent on L and in particular $\tau_d(k_v)$ grows with L. For the triangular barrier characterized by the field term F, it was shown that τ_d vanishes as κ^2, behavior in contrast to the rectangular barrier results. Insofar as the behavior of $\tau_i(k)$ and $\tau_d(k)$ mimic Eq. (11), as remains to be demonstrated, then the shape factor method readily gives the behaviors of their respective Gamow factors $\theta(E)$.

The data that support the findings of this study are available within the article.

ACKNOWLEDGMENTS

K.L.J. and A.S. gratefully acknowledge support from the NRL Naval Innovative Science and Engineering (NISE) program. D.A.S. and J.R. gratefully acknowledge support by the Air Force Office of Scientific Research (AFOSR) through the laboratory task 18RDCOR016, Cathode Materials Research for High Power Microwave Sources and the Air

Force Office of Scientific Research Chief Scientist Laboratory Research Initiative Request No. 99DE01COR. J.L.L. was supported by AFOSR under the Award No. FA9500-16-10037. R.S. gratefully acknowledges support from the AFRL Directed Energy Chief Scientist Office and the EOARD, Grant No. FA8655-20-1-7002.

[1] P. Zhang and Y. Y. Lau, J. Plasma Phys. **82**, 595820505 (2016).
[2] L. K. Ang and P. Zhang, Phys. Rev. Lett. **98**, 164802 (2007).
[3] M. Krüger, M. Schenk, M. Förster, and P. Hommelhoff, J. Phys. B: At., Mol. Opt. Phys. **45**, 074006 (2012).
[4] J.-W. Han, D.-I. Moon, and M. Meyyappan, Nano Lett. **17**, 2146 (2017).
[5] P. Zhang, S. Fairchild, T. Back, and Y. Luo, AIP Adv. **7**, 125203 (2017).
[6] Y. Zhou and P. Zhang, Phys. Rev. Research **2**, 043439 (2020).
[7] M. R. Bionta, F. Ritzkowsky, M. Turchetti, Y. Yang, D. Cattozzo Mor, W. P. Putnam, F. X. Kärtner, K. K. Berggren, and P. D. Keathley, Nat. Photonics **15**, 456 (2021).
[8] T. Rybka, M. Ludwig, M. F. Schmalz, V. Knittel, D. Brida, and A. Leitenstorfer, Nat. Photonics **10**, 667 (2016).
[9] P. Zhang, A. Valfells, L. K. Ang, J. W. Luginsland, and Y. Y. Lau, Appl. Phys. Rev. **4**, 011304 (2017).
[10] P. Hommelhoff, M. F. Kling, and M. I. Stockman, Ann. Phys. **525**, A13 (2013).
[11] A. S. Landsman and U. Keller, Phys. Rep. **547**, 1 (2015).
[12] D. Sokolovski and E. Akhmatskaya, Commun. Phys. **1**, 47 (2018).
[13] T. E. Hartman, J. Appl. Phys. **33**, 3427 (1962).
[14] L. A. MacColl, Phys. Rev. **40**, 621 (1932).
[15] M. Büttiker and R. Landauer, Phys. Rev. Lett. **49**, 1739 (1982).
[16] H. G. Winful, Phys. Rev. Lett. **91**, 260401 (2003).
[17] H. G. Winful, Phys. Rep. **436**, 1 (2006).
[18] K. L. Jensen, J. L. Lebowitz, J. M. Riga, D. A. Shiffler, and R. Seviour, Phys. Rev. B **103**, 155427 (2021).
[19] See, for example, Chap. 18 of Ref. [28].
[20] L. W. Nordheim, Proc. R. Soc. London, Ser. A **121**, 626 (1928).
[21] R. H. Fowler and L. Nordheim, Proc. R. Soc. London, Ser. A **119**, 173 (1928).
[22] R. Stratton, Proc. Phys. Soc., London, Sect. B **68**, 746 (1955).
[23] J. Petersen and E. Pollak, J. Phys. Chem. A **122**, 3563 (2018).
[24] L. Esaki, Rev. Mod. Phys. **46**, 237 (1974).
[25] E. Merzbacher, Phys. Today **55** (8), 44 (2002).
[26] K. L. Jensen and A. Ganguly, J. Appl. Phys. **73**, 4409 (1993).
[27] R. G. Forbes and J. H. B. Deane, Proc. R. Soc. London, Ser. A **463**, 2907 (2007).
[28] K. L. Jensen, *Introduction to the Physics of Electron Emission* (Wiley, Hoboken, NJ, 2017).
[29] T. Rivlin, E. Pollak, and R. S. Dumont, Phys. Rev. A **103**, 012225 (2021).
[30] K. Smith and G. Blaylock, Am. J. Phys. **85**, 763 (2017).
[31] V. Petrillo and V. Olkhovsky, Open Phys. **3**, 339 (2005).
[32] M. Cahay and S. Bandyopadhyay, *Problem Solving in Quantum Mechanics* (Wiley, Hoboken, NJ, 2017).
[33] K. L. Jensen, in *Wiley Encyclopedia of Electrical and Electronics Engineering*, edited by J. G. Webster (Wiley, New York, 2014), pp. 1–29.
[34] K. L. Jensen, D. Finkenstadt, D. A. Shiffler, A. Shabaev, S. G. Lambrakos, N. A. Moody, and J. J. Petillo, J. Appl. Phys. **123**, 065301 (2018).
[35] Y. Ando and T. Itoh, J. Appl. Phys. **61**, 1497 (1987).
[36] K. Brennan and C. Summers, J. Appl. Phys. **61**, 614 (1987).
[37] K. L. Jensen, J. M. Connelly, J. J. Petillo, J. R. Harris, S. Ovtchinnikov, A. J. Jensen, J. Burke, M. Cahay, J. Ludwick, G. Tripathi, J. Sanchez-Roddy, and D. Puentes, J. Appl. Phys. **129**, 095107 (2021).
[38] Observe that Ref. [26] mistakenly presents f with a square root in the exposition (not the calculations): It should be defined as $f \equiv 2mF/\hbar^2$ and have units of $(1/\mathrm{nm}^3)$.
[39] K. L. Jensen, IEEE Trans. Plasma Sci. **46**, 1881 (2018).
[40] J. H. B. Deane and R. G. Forbes, J. Phys. A: Math. Theor. **41**, 395301 (2008).